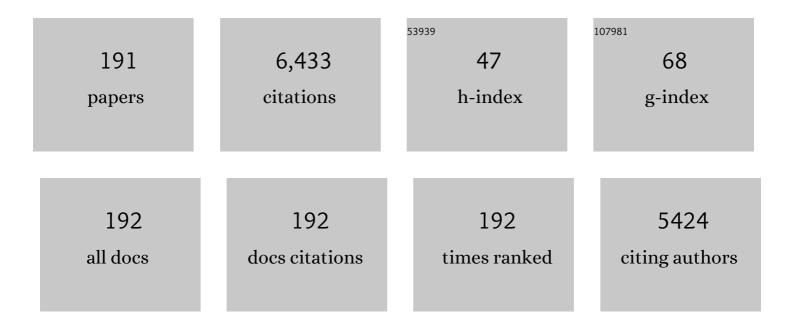
List of Publications by Year in descending order

Source: https://exaly.com/author-pdf/1737859/publications.pdf Version: 2024-02-01



Κε-ΟΠΙ CHEN

#	Article	IF	CITATIONS
1	Predicted stable high-pressure phases of copper-nitrogen compounds. Journal of Physics Condensed Matter, 2022, 34, 025401.	0.7	2
2	Quantum mechanical modeling of magnon-phonon scattering heat transport across three-dimensional ferromagnetic/nonmagnetic interfaces. Physical Review B, 2022, 105, .	1.1	39
3	Giant valley splitting in a MoTe <sub>2</sub> /MnSe <sub>2</sub> van der Waals heterostructure with room-temperature ferromagnetism. Materials Advances, 2022, 3, 2927-2933.	2.6	9
4	Nuclear Quantum Effects on the Charge-Density Wave Transition in NbX <sub>2</sub> (X = S, Se). Nano Letters, 2022, 22, 1858-1865.	4.5	7
5	Thermoelectric Conversion From Interface Thermophoresis and Piezoelectric Effects. Frontiers in Physics, 2022, 10, .	1.0	2
6	Nonequilibrium Green's function method for phonon heat transport in quantum system. Journal of Physics Condensed Matter, 2022, 34, 223001.	0.7	2
7	Perfect spin-filtering effect in molecular junctions based on half-metallic penta-hexa-graphene nanoribbons. Journal of Physics Condensed Matter, 2022, 34, 285302.	0.7	1
8	Evidence for moir $\tilde{A}$ © intralayer excitons in twisted WSe2/WSe2 homobilayer superlattices. Light: Science and Applications, 2022, 11, .	7.7	29
9	A first-principles study of exciton self-trapping and electric polarization in one-dimensional organic lead halide perovskites. Physical Chemistry Chemical Physics, 2022, 24, 17323-17328.	1.3	9
10	High tunneling magnetoresistance induced by symmetry and quantum interference in magnetic molecular junctions. Journal of Materials Chemistry C, 2021, 9, 5876-5884.	2.7	14
11	Magnetization textures in twisted bilayer <mmi:math xmlns:mml="http://www.w3.org/1998/Math/MathML"&gt; <mmi:mrow> <mmi:mi>Cr</mmi:mi> <mmi:msub> <mmi:mi mathvariant="normal"&gt;X <mmi:mn>3</mmi:mn> </mmi:mi </mmi:msub> </mmi:mrow>  () Tj ETQq1 :</mmi:math 	l ฏ <sub>3</sub> 78431	44ægBT ∕Ove
12	Nondegenerate Pâ€Type Inâ€Doped SnS <sub>2</sub> Monolayer Transistor. Advanced Electronic Materials, 2021, 7, 2001168.	2.6	13
13	Giant gauge factor of Van der Waals material based strain sensors. Nature Communications, 2021, 12, 2018.	5.8	62
14	Effect of out-of-plane strain on the phonon structures and anharmonicity of twisted multilayer graphene. Applied Physics Letters, 2021, 118, .	1.5	43
15	Tuning the Electrocatalytic Properties of Black and Gray Arsenene by Introducing Heteroatoms. ACS Omega, 2021, 6, 13124-13133.	1.6	7
16	Phaseâ€5elective Synthesis of Ultrathin FeTe Nanoplates by Controllable Fe/Te Atom Ratio in the Growth Atmosphere. Small, 2021, 17, 2101616.	5.2	13
17	A review of ultra-thin ferroelectric films. Journal of Physics Condensed Matter, 2021, 33, 403003.	0.7	8
	Cate controlled reversible restifying behavior investigated in a two dimensional symplemeth		

Gate-controlled reversible rectifying behavior investigated in a two-dimensional <mml:math xmlns:mml="http://www.w3.org/1998/Math/MathML"><mml:mrow><mml:msub><mml:mi>MoS</mml:mi><mml:mi>2</mm&#nn></mr diode. Physical Review B, 2021, 104, .

#	Article	IF	CITATIONS
19	Electrically controlled valley polarization in 2D buckled honeycomb structures. Modern Physics Letters B, 2021, 35, 2150390.	1.0	1
20	Tunable spin electronic and thermoelectric properties in twisted triangulene <b> <i>ï€</i> </b> -dimer junctions. Applied Physics Letters, 2021, 119, .	1.5	48
21	Thermoelectric Performance Enhanced by Destructive Quantum Interference in Nanoporous Carbon Nanotube Based Junctions. Physica Status Solidi - Rapid Research Letters, 2021, 15, 2100400.	1.2	3
22	The effects of covalent coupling strength on the electron transport properties and rectification in graphene/porphine/graphene molecular junctions. Physica E: Low-Dimensional Systems and Nanostructures, 2021, 134, 114867.	1.3	0
23	Magnetic properties manipulation of CrTe2 bilayer through strain and self-intercalation. Applied Physics Letters, 2021, 119, .	1.5	22
24	Toward a General Understanding of Exciton Self-Trapping in Metal Halide Perovskites. Journal of Physical Chemistry Letters, 2021, 12, 10472-10478.	2.1	38
25	Controllable anisotropic thermoelectric properties in 2D covalent organic radical frameworks. Applied Physics Letters, 2021, 119, .	1.5	16
26	Out-of-plane spontaneous polarization and superior photoelectricity in two-dimensional SiSn. Journal of Physics Condensed Matter, 2020, 32, 065003.	0.7	4
27	The electronic transport properties in graphyne and graphyne-like carbon-nitride nanoribbons. Journal Physics D: Applied Physics, 2020, 53, 055301.	1.3	Ο
28	Thermal Conductivity of Amorphous Materials. Advanced Functional Materials, 2020, 30, 1903829.	7.8	149
29	Nanoscale Organic Thermoelectric Materials: Measurement, Theoretical Models, and Optimization Strategies. Advanced Functional Materials, 2020, 30, 1903873.	7.8	97
30	Penta-Hexa-Graphene Nanoribbons: Intrinsic Magnetism and Edge Effect Induce Spin-Gapless Semiconducting and Half-Metallic Properties. ACS Applied Materials & Interfaces, 2020, 12, 53088-53095.	4.0	9
31	Excellent charge and spin transport in insulating hexagonal boron nitride with one-dimensional electron channel. Journal of Materials Chemistry C, 2020, 8, 17269-17276.	2.7	2
32	Switchable Spin Filters in Magnetic Molecular Junctions Based on Quantum Interference. Advanced Electronic Materials, 2020, 6, 2000689.	2.6	15
33	Design of Thermal Metamaterials with Excellent Thermal Control Functions by Using Functional Nanoporous Graphene. Physica Status Solidi - Rapid Research Letters, 2020, 14, 2000333.	1.2	7
34	Catalytic Performance of Two-Dimensional Bismuth Tuned by Defect Engineering for Nitrogen Reduction Reaction. Journal of Physical Chemistry C, 2020, 124, 19563-19570.	1.5	8
35	Thermal Transport in Two-Dimensional Heterostructures. Frontiers in Materials, 2020, 7, .	1.2	21
36	Exploring how hydrogen at gold–sulfur interface affects spin transport in single-molecule junction. Chinese Physics B, 2020, 29, 088503.	0.7	2

#	Article	IF	CITATIONS
37	Significantly enhanced thermoelectric performance of molecular junctions by the twist angle dependent phonon interference effect. Journal of Materials Chemistry A, 2020, 8, 11884-11891.	5.2	34
38	The coexistence of ferroelectricity and topological phase transition in monolayer <i>α</i> -In <sub>2</sub> Se <sub>3</sub> under strain engineering. Journal of Physics Condensed Matter, 2020, 32, 105501.	0.7	24
39	Chemically modified phosphorene as efficient catalyst for hydrogen evolution reaction. Journal of Physics Condensed Matter, 2020, 32, 025202.	0.7	13
40	Thermal transport of carbon nanomaterials. Journal of Physics Condensed Matter, 2020, 32, 153002.	0.7	94
41	Thermal Rectification in Asymmetric Graphene/Hexagonal Boron Nitride van der Waals Heterostructures. ACS Applied Materials & Interfaces, 2020, 12, 15517-15526.	4.0	55
42	α-Ag <sub>2</sub> S: A Ductile Thermoelectric Material with High <i>ZT</i> . ACS Omega, 2020, 5, 5796-5804.	1.6	64
43	Excellent thermoelectric performance induced by interface effect in MoS <sub>2</sub> /MoSe <sub>2</sub> van der Waals heterostructure. Journal of Physics Condensed Matter, 2020, 32, 055302.	0.7	43
44	Efficient strain modulation of 2D materials via polymer encapsulation. Nature Communications, 2020, 11, 1151.	5.8	215
45	Thermal Conductivity: Thermal Conductivity of Amorphous Materials (Adv. Funct. Mater. 8/2020). Advanced Functional Materials, 2020, 30, 2070048.	7.8	30
46	Organic Thermoelectric Materials: Nanoscale Organic Thermoelectric Materials: Measurement, Theoretical Models, and Optimization Strategies (Adv. Funct. Mater. 8/2020). Advanced Functional Materials, 2020, 30, 2070051.	7.8	3
47	Proton removal-induced positive and negative magnetoresistance in cobalt heme analogs. Journal of Materials Chemistry C, 2020, 8, 3758-3763.	2.7	4
48	Large Valley Splitting in van der Waals Heterostructures with Type-III Band Alignment. Physical Review Applied, 2020, 13, .	1.5	38
49	Direct Observation of the Linear Dichroism Transition in Two-Dimensional Palladium Diselenide. Nano Letters, 2020, 20, 1172-1182.	4.5	61
50	An efficient mechanism for enhancing the thermoelectricity of twin graphene nanoribbons by introducing defects. Physica E: Low-Dimensional Systems and Nanostructures, 2020, 122, 114160.	1.3	10
51	Excellent thermoelectric performance in weak-coupling molecular junctions with electrode doping and electrochemical gating. Science China: Physics, Mechanics and Astronomy, 2020, 63, 1.	2.0	51
52	Thermal transport properties in monolayer group-IV binary compounds. Journal of Physics Condensed Matter, 2020, 32, 305301.	0.7	10
53	Phase diagram and stability of mixed-cation lead iodide perovskites: A theory and experiment combined study. Physical Review Materials, 2020, 4, .	0.9	17
54	Pure spin current generated in thermally driven molecular magnetic junctions: a promising mechanism for thermoelectric conversion. Journal of Materials Chemistry A, 2019, 7, 19037-19044.	5.2	92

#	Article	IF	CITATIONS
55	Exploring high-performance anodes of Li-ion batteries based on the rules of pore-size dependent band gaps in porous carbon foams. Journal of Materials Chemistry A, 2019, 7, 21976-21984.	5.2	31
56	Prediction of intrinsic ferromagnetism in two-dimension planar metal-organic framework semiconductors. Journal of Magnetism and Magnetic Materials, 2019, 488, 165354.	1.0	17
57	Tuning the Catalytic Property of Phosphorene for Oxygen Evolution and Reduction Reactions by Changing Oxidation Degree. Journal of Physical Chemistry Letters, 2019, 10, 3440-3446.	2.1	43
58	Role of defects on the catalytic property of 2D black arsenic for hydrogen evolution reaction. Applied Physics Express, 2019, 12, 075502.	1.1	7
59	Electron transport properties of boron nitride chains between two-dimensional metallic borophene electrodes. Physica E: Low-Dimensional Systems and Nanostructures, 2019, 114, 113565.	1.3	7
60	Effect of electrophilic substitution and destructive quantum interference on the thermoelectric performance in molecular devices. Journal of Physics Condensed Matter, 2019, 31, 345303.	0.7	16
61	Bifunctional mechanism of N, P co-doped graphene for catalyzing oxygen reduction and evolution reactions. Journal of Chemical Physics, 2019, 150, 104701.	1.2	29
62	Abnormal diffusion behaviors of Cu atoms in van der Waals layered material MoS <sub>2</sub> . Journal of Materials Chemistry C, 2019, 7, 6052-6058.	2.7	18
63	Highly efficient thermal rectification in carbon/boron nitride heteronanotubes. Carbon, 2019, 148, 532-539.	5.4	44
64	Quantum transport properties of hybrid zigzag C <sub>3</sub> N and C <sub>3</sub> B nanoribbons. Journal Physics D: Applied Physics, 2019, 52, 185301.	1.3	1
65	Current Superposition Law Realized in Molecular Devices Connected in Parallel. Journal of Physical Chemistry C, 2019, 123, 10462-10468.	1.5	14
66	Charge Transport in Borophene: Role of Intrinsic Line Defects. Journal of Physical Chemistry C, 2019, 123, 6270-6275.	1.5	13
67	Synergy of tellurium and defects in control of activity of phosphorene for oxygen evolution and reduction reactions. Physical Chemistry Chemical Physics, 2019, 21, 22939-22946.	1.3	16
68	Tunable Schottky barrier width and enormously enhanced photoresponsivity in Sb doped SnS2 monolayer. Nano Research, 2019, 12, 463-468.	5.8	71
69	High Bipolar Conductivity and Robust Inâ€Plane Spontaneous Electric Polarization in Selenene. Advanced Electronic Materials, 2019, 5, 1800475.	2.6	32
70	The contaminant-induced instabilities of spin-transport properties in a MnPc-based spin valve. Organic Electronics, 2018, 58, 216-221.	1.4	5
71	The vertical growth of MoS2 layers at the initial stage of CVD from first-principles. Journal of Chemical Physics, 2018, 148, 134704.	1.2	18
72	Strain tuning of electronic properties of various dimension elemental tellurium with broken screw symmetry. Journal of Physics Condensed Matter, 2018, 30, 125001.	0.7	26

#	Article	IF	CITATIONS
73	Tunable thermal rectification in graphene/hexagonal boron nitride hybrid structures. Journal Physics D: Applied Physics, 2018, 51, 085103.	1.3	23
74	Nanoporous carbon foam structures with excellent electronic properties predicted by first-principles studies. Carbon, 2018, 129, 809-818.	5.4	23
75	A nearly perfect spin filter and a spin logic gate based on a porphyrin/graphene hybrid material. Physical Chemistry Chemical Physics, 2018, 20, 3997-4004.	1.3	31
76	Tuning transport performance in two-dimensional metal-organic framework semiconductors: Role of the metal <i>d</i> band. Applied Physics Letters, 2018, 112, .	1.5	53
77	Nanoscale thermal transport: Theoretical method and application. Chinese Physics B, 2018, 27, 036304.	0.7	21
78	Anisotropic thermal conductivity in carbon honeycomb. Journal of Physics Condensed Matter, 2018, 30, 155702.	0.7	15
79	Covalent coupling of porphines to graphene edges: Quantum transport properties and their applications in electronics. Carbon, 2018, 127, 611-617.	5.4	47
80	Spin gapless semiconductor and half-metal properties in magnetic penta-hexa-graphene nanotubes. Organic Electronics, 2018, 63, 310-317.	1.4	28
81	A local resonance mechanism for thermal rectification in pristine/branched graphene nanoribbon junctions. Applied Physics Letters, 2018, 113, .	1.5	72
82	Metal and ligand effects on the stability and electronic properties of crystalline two-dimensional metal-benzenehexathiolate coordination compounds. Journal of Physics Condensed Matter, 2018, 30, 465301.	0.7	20
83	An efficient mechanism for enhancing the thermoelectricity of nanoribbons by blocking phonon transport in 2D materials. Journal of Physics Condensed Matter, 2018, 30, 275701.	0.7	28
84	<i>Ab initio</i> study of the moisture stability of lead iodine perovskites. Journal of Physics Condensed Matter, 2018, 30, 355501.	0.7	10
85	Edge-oxidation effects on the thermoelectric properties in graphene nanoribbons. Physica E: Low-Dimensional Systems and Nanostructures, 2018, 104, 302-308.	1.3	8
86	Hydrogen induced contrasting modes of initial nucleations of graphene on transition metal surfaces. Journal of Chemical Physics, 2017, 146, 034704.	1.2	4
87	Excellent Thermoelectric Properties in monolayer WSe2 Nanoribbons due to Ultralow Phonon Thermal Conductivity. Scientific Reports, 2017, 7, 41418.	1.6	36
88	Huge magnetoresistance induced by half-metal–semiconductor phase transition in a one-dimensional spin chain: a first-principles study. Physical Chemistry Chemical Physics, 2017, 19, 9417-9423.	1.3	8
89	A wave-dominated heat transport mechanism for negative differential thermal resistance in graphene/hexagonal boron nitride heterostructures. Applied Physics Letters, 2017, 110, .	1.5	63
90	An important rule for realizing metal → half-metal → semiconductor transition in single-molecule junctions. Journal Physics D: Applied Physics, 2017, 50, 215102.	1.3	8

#	Article	IF	CITATIONS
91	Effects of electron-phonon interactions on the spin-dependent Seebeck effect in graphene nanoribbons. Carbon, 2017, 119, 548-554.	5.4	20
92	Huge inelastic current at low temperature in graphene nanoribbons. Journal of Physics Condensed Matter, 2017, 29, 075301.	0.7	12
93	Breaking surface states causes transformation from metallic to semi-conducting behavior in carbon foam nanowires. Carbon, 2017, 111, 867-877.	5.4	20
94	Seeking the Dirac cones in the MoS2/WSe2 van der Waals heterostructure. Applied Physics Letters, 2017, 111, 171602.	1.5	31
95	The length and hydrogenation effects on electronic transport properties of carbon-based molecular wires. Organic Electronics, 2017, 51, 332-340.	1.4	13
96	Effect of room temperature lattice vibration on the electron transport in graphene nanoribbons. Applied Physics Letters, 2017, 111, 133107.	1.5	53
97	Anomalous thermal anisotropy of two-dimensional nanoplates of vertically grown MoS2. Applied Physics Letters, 2017, 111, .	1.5	8
98	Excellent thermoelectric properties induced by different contact geometries in phenalenyl-based single-molecule devices. Scientific Reports, 2017, 7, 10842.	1.6	19
99	Large anisotropic thermal conductivity and excellent thermoelectric properties observed in carbon foam. Journal of Applied Physics, 2017, 122, .	1.1	11
100	Large spin rectifying and high-efficiency spin-filtering in superior molecular junction. Organic Electronics, 2017, 50, 184-190.	1.4	22
101	Thermal conductance of electrons in graphene and stanene ribbons modulated via electron-phonon coupling. Journal of Applied Physics, 2017, 122, .	1.1	9
102	Strong interfacial interaction and enhanced optical absorption in graphene/InAs and MoS <sub>2</sub> /InAs heterostructures. Journal of Materials Chemistry C, 2017, 5, 9429-9438.	2.7	32
103	Influence of anchoring groups on single-molecular junction conductance: Theoretical comparative study of thiol and amine. Organic Electronics, 2017, 50, 198-203.	1.4	11
104	Half-metallicity and high spin-filtering effect of magnetic atoms embedded zigzag 6, 6, 12-graphyne nanoribbon. Carbon, 2017, 113, 170-175.	5.4	24
105	Thermal Transport of Flexural and In-Plane Phonons Modulated by Bended Graphene Nanoribbons. Journal of Nanomaterials, 2016, 2016, 1-7.	1.5	3
106	Electronic Structures of Free-Standing Nanowires made from Indirect Bandgap Semiconductor Gallium Phosphide. Scientific Reports, 2016, 6, 28240.	1.6	13
107	Phonon wave interference in graphene and boron nitride superlattice. Applied Physics Letters, 2016, 109, 023101.	1.5	94
108	Triggering piezoelectricity directly by heat to produce alternating electric voltage. Applied Physics Letters, 2016, 109, .	1.5	13

#	Article	IF	CITATIONS
109	Interesting odd-even rules of spin-filtering and magnetoresistance effects in a single-molecule spintronic device. Carbon, 2016, 104, 20-26.	5.4	20
110	Hydrogen tautomerization: A simple approach to tune spin-filtering effects in a quinone-based spintronic device. Organic Electronics, 2016, 35, 12-16.	1.4	8
111	Resonant Charge Transport in Conjugated Molecular Wires beyond 10 nm Range. Journal of the American Chemical Society, 2016, 138, 11140-11143.	6.6	71
112	Significant decrease in thermal conductivity of multi-walled carbon nanotube induced by inter-wall van der Waals interactions. Physics Letters, Section A: General, Atomic and Solid State Physics, 2016, 380, 1861-1864.	0.9	29
113	Thermal rectification and negative differential thermal resistance behaviors in graphene/hexagonal boron nitride heterojunction. Carbon, 2016, 100, 492-500.	5.4	108
114	The thermal conductivity in hybridised graphene and boron nitride nanoribbons modulated with strain. Journal Physics D: Applied Physics, 2016, 49, 115301.	1.3	21
115	Spin filtering and rectifying effects in the zinc methyl phenalenyl molecule between graphene nanoribbon leads. Organic Electronics, 2016, 28, 244-251.	1.4	57
116	First-Principles Determination of Ultralow Thermal Conductivity of monolayer WSe2. Scientific Reports, 2015, 5, 15070.	1.6	78
117	Comparison on thermal transport properties of graphene and phosphorene nanoribbons. Scientific Reports, 2015, 5, 16215.	1.6	14
118	Conjunction of standing wave and resonance in asymmetric nanowires: a mechanism for thermal rectification and remote energy accumulation. Scientific Reports, 2015, 5, 17525.	1.6	20
119	Remote p-type Doping in GaSb/InAs Core-shell Nanowires. Scientific Reports, 2015, 5, 10813.	1.6	11
120	Enhancement of thermoelectric performance in β-graphyne nanoribbons by suppressing phononic thermal conductance. Carbon, 2015, 85, 24-27.	5.4	76
121	Reversible switching in gold-atom–organic-molecule complex induced by reversible bond formation. Organic Electronics, 2015, 18, 101-106.	1.4	29
122	Rectifying behavior and negative differential resistance in triangular graphene p–n junctions induced by vertex B–N mixture doping. Organic Electronics, 2015, 19, 92-97.	1.4	57
123	Designing multi-functional devices based on two benzene rings molecule modulated with Co and N atoms. Organic Electronics, 2015, 23, 133-137.	1.4	50
124	Abnormal oscillatory conductance and strong odd–even dependence of a perfect spin-filtering effect in a carbon chain-based spintronic device. Journal of Materials Chemistry C, 2015, 3, 5697-5702.	2.7	50
125	Influence of boundary types on rectifying behaviors in hexagonal boron-nitride/graphene nanoribbon heterojunctions. Organic Electronics, 2015, 27, 137-142.	1.4	39
126	Effect of length and negative differential resistance behavior in conjugated molecular wire tetrathiafulvalene devices. Modern Physics Letters B, 2015, 29, 1550106.	1.0	3

#	Article	IF	CITATIONS
127	Characteristics of classical Kirchhoff's superposition law inÂcarbonÂatomic wires connected in parallel. Carbon, 2015, 95, 503-510.	5.4	27
128	The effect of oxygen vacancy on holes-induced d0 magnetism in CaTiO3 and CaZrO3. Modern Physics Letters B, 2015, 29, 1550137.	1.0	3
129	The enhancement of the thermoelectric performance in zigzag graphene nanoribbon by edge states. Carbon, 2015, 94, 942-945.	5.4	13
130	Enhancement of thermoelectric performance in InAs nanotubes by tuning quantum confinement effect. Journal of Applied Physics, 2014, 115, .	1.1	17
131	An important mechanism for thermal rectification in graded nanowires. Applied Physics Letters, 2014, 105, .	1.5	65
132	The effects of the chemical composition and strain on the electronic properties of GaSb/InAs core-shell nanowires. Journal of Applied Physics, 2014, 116, 094308.	1.1	24
133	Phonon scattering and thermal conductance properties in two coupled graphene nanoribbons modulated with bridge atoms. Physics Letters, Section A: General, Atomic and Solid State Physics, 2014, 378, 1952-1955.	0.9	8
134	Spin filtering effect and magnetoresistance in zigzag 6, 6, 12-graphyne nanoribbon system. Carbon, 2014, 76, 175-182.	5.4	51
135	High-vacuum tip enhanced Raman spectroscopy. Frontiers of Physics, 2014, 9, 17-24.	2.4	14
136	Magnetic configuration dependence of magnetoresistance in a Fe-porphyrin-like carbon nanotube spintronic device. Applied Physics Letters, 2014, 104, 033104.	1.5	55
137	Enhance the stability of α-graphyne nanoribbons by dihydrogenation. Organic Electronics, 2014, 15, 3392-3398.	1.4	35
138	Negative differential resistance induced by the Jahn–Teller effect in single molecular coulomb blockade devices. Computational Materials Science, 2014, 82, 33-36.	1.4	42
139	Thermal conductance associated with six types of vibration modes in quantum wire modulated with quantum dot. Physics Letters, Section A: General, Atomic and Solid State Physics, 2014, 378, 2195-2200.	0.9	2
140	Thermal transport for flexural and in-plane phonons in graphene nanoribbons. Carbon, 2014, 77, 360-365.	5.4	23
141	Stable Two-Dimensional Conductance Switch of Polyaniline Molecule Connecting to Graphene Nanoribbons. Scientific Reports, 2014, 4, 5976.	1.6	26
142	Enhancement of Thermoelectric Performance by Reducing Phonon Thermal Conductance in Multiple Core-shell Nanowires. Scientific Reports, 2014, 4, 7150.	1.6	42
143	Effect of pentagon–heptagon defect on thermal transport properties in graphene nanoribbons. Carbon, 2013, 65, 181-186.	5.4	53
144	Enhance ferromagnetism by stabilizing the cation vacancies in GaN. European Physical Journal B, 2013, 86, 1.	0.6	7

#	Article	IF	CITATIONS
145	Phonon thermal transport in InAs nanowires with different size and growth directions. Physics Letters, Section A: General, Atomic and Solid State Physics, 2013, 377, 3144-3147.	0.9	35
146	Giant magnetoresistance effect and spin filters in phthalocyanine-based molecular devices. Organic Electronics, 2013, 14, 2940-2947.	1.4	70
147	Controllable unzipping for intramolecular junctions of graphene nanoribbons and single-walled carbon nanotubes. Nature Communications, 2013, 4, 1374.	5.8	125
148	Spin filtering, magnetic and electronic switching behaviors in manganese porphyrin-based spintronic devices. Journal of Materials Chemistry C, 2013, 1, 4014.	2.7	94
149	Heat generated by electrical current in a mesoscopic system perturbed by alternating current fields. Journal of Applied Physics, 2013, 114, .	1.1	33
150	Core-shell nanowire serves as heat cable. Applied Physics Letters, 2013, 103, .	1.5	27
151	Controllable low-bias negative differential resistance and rectifying behaviors induced by symmetry breaking. Applied Physics Letters, 2013, 102, .	1.5	30
152	Ballistic thermoelectric properties in boron nitride nanoribbons. Journal of Applied Physics, 2013, 114, 144311.	1.1	17
153	Optical transport through finite superlattice modulated with three-component quasiperiodic defect. Journal of Applied Physics, 2012, 112, 043524.	1.1	0
154	Strong current polarization and negative differential resistance in chiral graphene nanoribbons with reconstructed (2,1)-edges. Applied Physics Letters, 2012, 101, 073101.	1.5	15
155	Ballistic thermal transport contributed by the in-plane waves in a quantum wire modulated with an acoustic nanocavity. Journal of Applied Physics, 2012, 112, 124315.	1.1	1
156	PERFECT OPTICAL TRANSPORT AND OPTICAL BAND GAP IN QUASIPERIODIC SUPERLATTICES. Modern Physics Letters B, 2012, 26, 1250110.	1.0	0
157	The weak Ï€ â^' Ï€ interaction originated resonant tunneling and fast switching in the carbon based electronic devices. AIP Advances, 2012, 2, 012137.	0.6	8
158	Ballistic thermoelectric properties in graphene-nanoribbon-based heterojunctions. Applied Physics Letters, 2012, 101, .	1.5	49
159	Enhancement of thermoelectric properties in graphene nanoribbons modulated with stub structures. Applied Physics Letters, 2012, 100, .	1.5	78
160	Symmetry of atomistic structure for armchair-edge graphene nanoribbons under uniaxial strain. Applied Physics Letters, 2012, 100, 153112.	1.5	14
161	Nonlinear phonon transport and ballistic thermal rectification in asymmetric graphene-based three terminal junctions. Applied Physics Letters, 2012, 100, .	1.5	41
162	Design of Graphene-Nanoribbon Heterojunctions from First Principles. Journal of Physical Chemistry C, 2011, 115, 12616-12624.	1.5	49

#	Article	IF	CITATIONS
163	Edge Hydrogenation-Induced Spin-Filtering and Rectifying Behaviors in the Graphene Nanoribbon Heterojunctions. Journal of Physical Chemistry C, 2011, 115, 25072-25076.	1.5	180
164	Nitrogen doping-induced rectifying behavior with large rectifying ratio in graphene nanoribbons device. Journal of Applied Physics, 2011, 109, .	1.1	81
165	Tuning the Electronic Transport Properties of Zigzag Graphene Nanoribbons via Hydrogenation Separators. Journal of Physical Chemistry C, 2011, 115, 24366-24372.	1.5	10
166	Ballistic thermal conductance in graphene nanoribbon with double-cavity structure. Applied Physics Letters, 2011, 99, .	1.5	31
167	Thermal transport by phonons in zigzag graphene nanoribbons with structural defects. Journal of Physics Condensed Matter, 2011, 23, 315302.	0.7	60
168	Donor-donor binding in In2O3: Engineering shallow donor levels. Journal of Applied Physics, 2010, 107, 083704.	1.1	21
169	Quantized thermal conductance at low temperatures in quantum wire with catenoidal contacts. Physical Review B, 2010, 81, .	1.1	44
170	Mechanically and electronically controlled molecular switch behavior in a compound molecular device. Applied Physics Letters, 2010, 97, 103506.	1.5	16
171	LOCALIZED WANNIER EXCITON IN DEFECT LAYER EMBEDDED BETWEEN TWO SEMI-INFINITE SUPERLATTICES. International Journal of Modern Physics B, 2010, 24, 3501-3511.	1.0	0
172	Negative differential resistance and rectifying behaviors in phenalenyl molecular device with different contact geometries. Applied Physics Letters, 2010, 96, .	1.5	166
173	Electronic transport properties in a bimolecular device modulated with different side groups. Journal of Applied Physics, 2010, 107, .	1.1	25
174	Transition from insulator to metal induced by hybridized connection of graphene and boron nitride nanoribbons. Applied Physics Letters, 2010, 97, .	1.5	135
175	Tuning intermolecular non-covalent interactions for nanowires of organic semiconductors. Nanoscale, 2010, 2, 2652.	2.8	24
176	Nanomechanically induced molecular conductance switch. Applied Physics Letters, 2009, 95, 232118.	1.5	14
177	Effects of dimensionality on the ballistic phonon transport and thermal conductance in nanoscale structures. Journal of Applied Physics, 2009, 105, 114318.	1.1	8
178	Electronic transport properties in doped C60 molecular devices. Applied Physics Letters, 2009, 94, .	1.5	81
179	THERMAL TRANSPORT BY BALLISTIC PHONON IN A SEMICONDUCTOR RECTANGULAR QUANTUM WIRE MODULATED WITH QUANTUM DOT. Modern Physics Letters B, 2009, 23, 3597-3607.	1.0	1
180	Transitions between semiconductor and metal induced by mixed deformation in carbon nanotube devices. Applied Physics Letters, 2009, 94, .	1.5	28

#	Article	IF	CITATIONS
181	Thermal transport associated with ballistic phonons in asymmetric quantum structures. Frontiers of Physics in China, 2009, 4, 420-425.	1.0	3
182	Theoretical investigation of the negative differential resistance in squashed C60 molecular device. Applied Physics Letters, 2008, 92, .	1.5	97
183	EFFECTS OF STRUCTURAL AND CENTRAL METAL IONS MODIFICATION ON THE ELECTRONIC TRANSPORT PROPERTIES OF PORPHYRIN MOLECULAR JUNCTIONS. Modern Physics Letters B, 2008, 22, 661-670.	1.0	6
184	Effect of the evanescent modes on ballistic thermal transport in quantum structures. Journal of Applied Physics, 2008, 103, 084501.	1.1	26
185	Negative differential resistance behaviors in porphyrin molecular junctions modulated with side groups. Applied Physics Letters, 2008, 92, .	1.5	77
186	Acoustic phonon transport and ballistic thermal conductance through a three-dimensional double-bend quantum structure. Journal of Applied Physics, 2008, 104, 054312.	1.1	17
187	Ballistic thermal conductance in a three-dimensional quantum wire modulated with stub structure. Applied Physics Letters, 2007, 90, 193502.	1.5	49
188	Effect of length and size of heterojunction on the transport properties of carbon-nanotube devices. Applied Physics Letters, 2007, 91, 133511.	1.5	109
189	Effect of defects on the thermal conductivity in a nanowire. Physical Review B, 2005, 72, .	1.1	105
190	Effects of Intermolecular Interaction and Moleculeâ^'Electrode Couplings on Molecular Electronic Conductance. Journal of Physical Chemistry B, 2005, 109, 12304-12308.	1.2	53
191	Localized folded acoustic phonon modes in coupled superlattices with structural defects. Physical Review B, 2000, 61, 12075-12081.	1.1	50